

Pattern-Potential-Guided Growth of Textured Macromolecular Films on Graphene/High-Index Copper

Dikui Zhou, Zhihong Zhang, Yihan Zhu, Yiqun Xiao, Qingqing Ding, Luoyuan Ruan, Yiran Sun, Zhibin Zhang, Chongzhi Zhu, Zongping Chen, Yongjun Wu, Yuhui Huang, Guan Sheng, Jixue Li, Dapeng Yu, Enge Wang, Zhaohui Ren,* Xinhui Lu,* Kaihui Liu,* and Gaorong Han*

Macromolecular films are crucial functional materials widely used in the fields of mechanics, electronics, optoelectronics, and biology, due to their superior properties of chemical stability, small density, high flexibility, and solution-processing ability. Their electronic and mechanical properties, however, are typically much lower than those of crystalline materials, as the macromolecular films have no long-range structural ordering. The state-of-the-art for producing highly ordered macromolecular films is still facing a great challenge due to the complex interactions between adjacent macromolecules. Here, the growth of textured macromolecular films on a designed graphene/high-index copper (Cu) surface is demonstrated. This successful growth is driven by a patterned potential that originates from the different amounts of charge transfer between the graphene and Cu surfaces with, alternately, terraces and step edges. The textured films exhibit a remarkable improvement in remnant ferroelectric polarization and fracture strength. It is also demonstrated that this growth mechanism is universal for different macromolecules. As meter-scale graphene/high-index Cu substrates have recently become available, the results open a new regime for the production and applications of highly ordered macromolecular films with obvious merits of high production and low cost.

Functional macromolecules, such as ferroelectric polymers, biomolecules, hybrid perovskite, liquid crystals, and synthetic polymers, have demonstrated fascinating functionalities in biology, mechanics, and electronics.^[1–8] An approach to control the configurations and arrangements of macromolecules is highly promising for the improved functionalities by constructing ordered materials at different scales.^[6–9] In particular, the special polar groups or units in most macromolecules, which can generate charged surfaces, hydrogen bonding, and oriented dipoles, have been determined to be crucial for the functionalities.^[10] However, the strong electrostatic interactions between polar groups or units, together with an irregular space configuration of the long molecular chains, always lead to a big challenge in fabricating highly ordered macromolecular materials. Over the past decades, different strategies

D. K. Zhou, L. Y. Ruan, Y. R. Sun, Prof. Z. P. Chen, Prof. Y. J. Wu,
Dr. Y. H. Huang, Prof. Z. H. Ren, Prof. G. R. Han
State Key Laboratory of Silicon Materials
School of Materials Science and Engineering
Cyrus Tang Center for Sensor Materials and Application
Zhejiang University
Hangzhou 310027, China
E-mail: renzh@zju.edu.cn; hgr@zju.edu.cn

Dr. Z. H. Zhang, Z. B. Zhang, Prof. E. G. Wang, Prof. K. H. Liu
State Key Lab for Mesoscopic Physics
Frontiers Science Center for Nano-optoelectronics
International Center for Quantum Materials
Collaborative Innovation Center of Quantum Matter
School of Physics
Peking University
Beijing 100871, China
E-mail: khliu@pku.edu.cn

Prof. Y. H. Zhu, Prof. C. Z. Zhu
Center for Electron Microscopy
State Key Laboratory Breeding Base of Green Chemistry
Synthesis Technology and College of Chemical Engineering
Zhejiang University of Technology
Hangzhou 310014, China


Y. Q. Xiao, Prof. X. H. Lu
Department of Physics
The Chinese University of Hong Kong
New Territories, Hong Kong 999077, China
E-mail: xinhui.lu@cuhk.edu.hk

Dr. Q. Q. Ding, Prof. J. X. Li
State Key Laboratory of Silicon Materials
and Center of Electron Microscopy
School of Materials Science and Engineering
Zhejiang University
Hangzhou 310027, China

Dr. Y. H. Huang, Prof. Z. H. Ren
Research Center for Intelligent Sensing
Zhejiang Lab
Hangzhou 311100, China

Prof. G. Sheng
Advanced Membranes and Porous Materials Center
Physical Science and Engineering
King Abdullah University of Science and Technology
Thuwal 23955-6900, Kingdom of Saudi Arabia

Prof. D. P. Yu
Shenzhen Institute for Quantum Science and Engineering
Southern University of Science and Technology
Shenzhen 518055, China

 The ORCID identification number(s) for the author(s) of this article can be found under <https://doi.org/10.1002/adma.202006836>.

DOI: 10.1002/adma.202006836

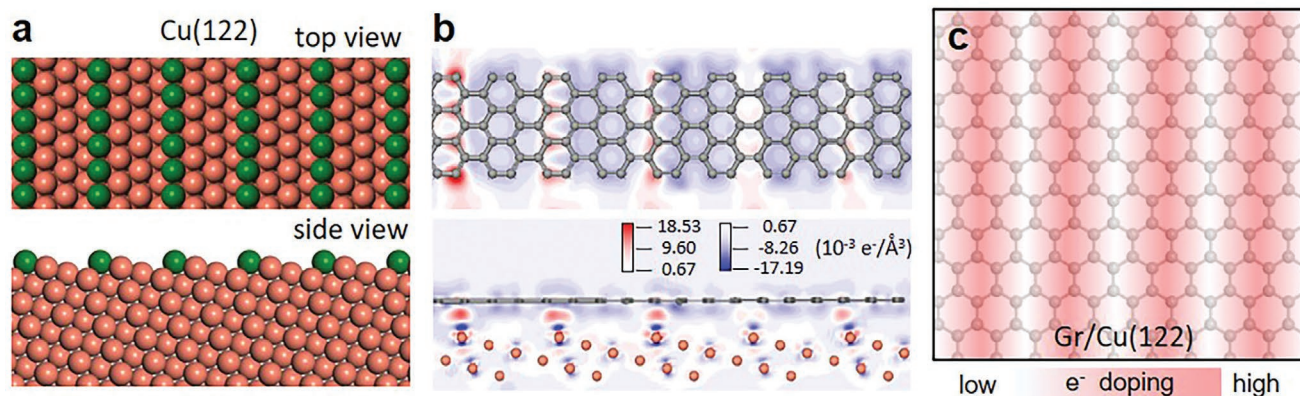


Figure 1. Predicted patterned potential distribution in graphene/Cu(122) from DFT calculations. a) Schematic atomic structure of ideal Cu(122), and the green atoms represent the step edges of Cu surface. b) DFT calculations of charge density at graphene/Cu(122) interface from top and side views, respectively. The red and blue represent accumulation and depletion regions of electrons, respectively. c) Schematic of electron distribution in graphene on Cu(122) based on DFT calculations.

have been developed for preparing the ordered macromolecular films, which can mainly be achieved by: i) confinement space via the Langmuir–Blodgett technique,^[11] template method,^[7] and nanoimprint lithography;^[12] ii) designed fluid-flow in solution-coating technique;^[13] iii) external force, electric, and magnetic fields.^[8] Nevertheless, these approaches remain largely process and material dependent, where a scalability and generality cannot be achieved simultaneously.

Atomically well-defined surface is an ideal platform that can direct atoms and molecules to arrange into a geometric order by van der Waals interaction.^[14] Toward this, 2D materials, such as graphene and hexagonal boron nitride (h-BN), serving as substrates to tailor the molecular configurations and arrangements, have been widely investigated.^[15,16] The successful synthesis of large-area single-crystal graphene and h-BN films provides the possibility to realize the preparation of ordered macromolecular films at large scales.^[17–19] Recently, large-size single-crystal copper (Cu) foils with various high-index facets have been produced, and the epitaxy of single-crystal graphene and h-BN on them demonstrated as well.^[20] Interestingly, graphene grown on high-index copper surface is able to generate 1D superlattices, modulating the electronic structures of the graphene.^[21] Moreover, charge transfer usually occurs when graphene contacts with copper, due to their different work functions.^[22] These results forebode that 1D electronic potential could be constructed in the system of graphene/high-index copper foil, which is particularly desirable for organization of polar macromolecules.^[23] For this consideration, graphene/Cu(122) has been well investigated in this work. An ideal Cu(122) facet is composed of atomic steps as schematically shown in **Figure 1a**. Such geometric corrugation of Cu(122) is expected to interact with graphene differently at step edges and on the terrace.^[24] To validate this, we employed density functional theory (DFT) calculations to estimate the charge distribution at the graphene/Cu(122) interface. The charge transfer between copper and graphene originates from weak chemisorption, which stems from the upward shift of Fermi level with respect to the conical point of graphene, leading to n-type doping of graphene with electrons as the major carriers. Such doping is strongly altered by

interface dipoles arising from a direct short-range metal–graphene interaction. The step edges therefore donate more electrons (green Cu atoms in **Figure 1a**, $\approx 1.8 \times 10^{-2} \text{ e}^- \text{ \AA}^{-3}$) to graphene than step terraces ($\approx 6.7 \times 10^{-4} \text{ e}^- \text{ \AA}^{-3}$) due to the smaller distance and stronger interaction between step edges and graphene,^[22] leading to a local charge density gradient and thus a patterned potential on the substrate surface (**Figure 1b,c**).

Experimentally, we chose ferroelectric poly(vinylidene fluoride-co-trifluoroethylene) (P(VDF-TrFE)) with macromolecules stability as a model system to investigate macromolecular chains arrangements on the graphene/Cu(122) substrate. Employing a carefully designed thermal annealing technique,^[20] we deliberately fabricated large-size single-crystal Cu(122) substrate and then grew graphene on it. The characterization results of electron backscattered diffraction (EBSD) and X-ray diffraction (XRD) of the Cu substrate also verified its (122) facet nature, and high-quality monolayer graphene grown on Cu(122) was characterized by Raman spectrum (**Figure S1a–c**, Supporting Information). The growth of graphene induces step bunching of a vicinal Cu(122) surface with alternating (122) and (111) facets to relax the compression strain as reported previously,^[25] supported by transmission electron microscopy and atomic force microscopy (AFM) results (**Figure S1d–f**, Supporting Information). P(VDF-TrFE) macromolecules adopt dipoles, generated by opposite $-\text{CH}_2$ and $-\text{CF}_2$ groups perpendicular to the carbon backbone chains, which usually crystallize into randomly arranged lamellae with polymer chains aligning parallel to lamellae normal.^[6] Meanwhile, we also prepared the macromolecular films on bare Cu(122) (atomically stepped surface) and graphene/Cu(111) (uniform interface charge transfer). In a general preparation process, the P(VDF-TrFE) dissolved in tetrahydrofuran was first spin-coated onto substrates and then annealed in vacuum at 180 °C, where the film was molten (**Figure S2**, Supporting Information) and finally cooled down to room temperature slowly. Scanning electron microscopy (SEM) images showed that after annealing P(VDF-TrFE) film on graphene/Cu(122) substrate possessed distinct textured structure, consisting of highly oriented strips with widths of about 500 nm (**Figure 2a**; **Figure S3a**, Supporting Information). The

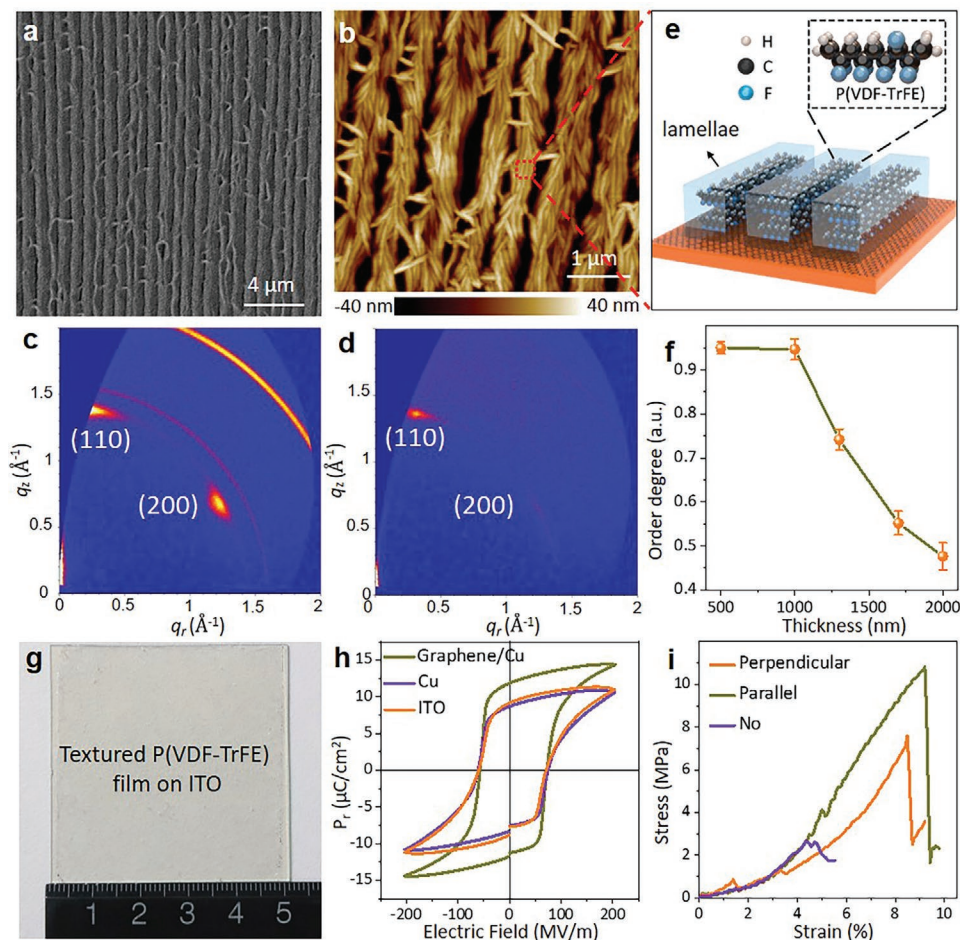


Figure 2. Characterization of highly oriented P(VDF-TrFE) films grown on graphene/Cu(122) substrate. a) SEM and b) AFM images of the textured P(VDF-TrFE) film. c,d) GIWAXS profiles of the highly oriented P(VDF-TrFE) film with in-plane rotational angles of 0° (c) and 90° (d), respectively. e) Schematic of the arrangement of P(VDF-TrFE) molecular chains on graphene/Cu(122) substrate. f) Order degree of P(VDF-TrFE) films with different thickness, counted by the ratio of the lamellae parallel to the orientation direction of the film. g) P(VDF-TrFE) textured film transferred onto indium tin oxide (ITO) glass. h) Ferroelectric hysteresis loops of P(VDF-TrFE) films grown on different substrates tested with bottom electrodes of ITO. i) Stress-strain curves for the textured P(VDF-TrFE) films with stress loading parallelly (green) and perpendicularly (orange) to the orientation of strips, and the no-textured film, respectively.

more detailed AFM result revealed the strips were composed of aligned lamellae with ≈ 100 nm in thickness, ≈ 1 μm in length (Figure 2b), allowing a preliminary conclusion that graphene/Cu(122) substrate could guide the arrangements of the macromolecular chains. In comparison, the films on Cu(122) and graphene/Cu(111) were consisted of randomly oriented lamellae (Figure S3b,c, Supporting Information). The above results consolidated that a patterned potential on the substrate surface is the key to direct the textured structure of the macromolecule, but not atomically stepped surface or interface charge transfer.

Such textured films were characterized by XRD to show only one diffraction peak at 19.8° , corresponding to that of (110)/(200) planes in the β -phase of P(VDF-TrFE) (Figure S5a, Supporting Information, JCPDS 42-1649^[26]), where the lattice spacing for (110) and (200) is almost equal. Furthermore, the grazing-incidence wide-angle X-ray scattering (GIWAXS) technique was employed to determine the molecular packing within these stripes. When X-rays impinged perpendicular to the direction of the strips, two bright diffraction spots on the arc of $|q| \approx 1.4 \text{ \AA}^{-1}$

were observed, corresponding to the reflection of (110) and (200) planes, consistent with the XRD results; when the sample was rotated 90° in-plane so that X-rays became parallel to the strip direction, the diffraction spot on meridian remained but the other spot almost disappeared (Figure 2c,d; Figure S4, Supporting Information). These GIWAXS results confirm the highly ordered lamellae structure and suggest that the stacking of P(VDF-TrFE) molecular chains is normal to the strip direction, as schematically illustrated in Figure 2e. Moreover, we have used SEM images to investigate the ordering behaviors of P(VDF-TrFE) films with different thickness on the graphene/Cu(122) substrates. The results showed that the lamellae remained well ordered in the film with a thickness up to 1000 nm, demonstrating that the induction from the substrate to the macromolecular chains arrangements is of long-range interaction, while above this critical thickness the order degree decreases with increase of thickness (Figure 2f; Figure S5, Supporting Information).

All above results verify that the graphene/Cu(122) substrate can induce the ordered arrangements and configurations of

P(VDF-TrFE) macromolecules and thus the formation of the textured films. The thick textured film is capable of being self-supporting after the substrate being removed and its area is subjected to the substrate size (a $5 \times 5 \text{ cm}^2$ film shown in Figure 2g). More importantly, the textured film possessed a remarkable improvement in remnant ferroelectric polarization ($11.8 \mu\text{C cm}^{-2}$) compared to those no-textured ones ($8.6 \mu\text{C cm}^{-2}$) (Figure 2h). Meanwhile, the film exhibited an anisotropic mechanical property, that the strength along the stripe direction is $\approx 50\%$ higher than that perpendicular to the stripe direction, and distinct fracture strength enhancement (from 2.5 to 10.8 MPa) (Figure 2i; Figure S6, Supporting Information). These achievements make this film highly attractive for flexible electric device applications.^[27]

To understand the formation mechanism of textured films on graphene/Cu(122) substrate, in situ SEM characterization was performed to study the evolution process in real time. First, at the temperature of $160 \text{ }^\circ\text{C}$, no clear morphology contrast could be observed because P(VDF-TrFE) film was molten (Figure 3a). When the temperature was lowered to below the crystallizing point ($135 \text{ }^\circ\text{C}$, Figure S2, Supporting Information), lamellae structure started to form with some small ordered regions embedded in random oriented ones (Figure 3b; Figure S7, Supporting Information). As temperature further declined, the ordered areas grew quickly by merging nearby randomly oriented lamellae (Figure 3c). When it was cooled down to room temperature ($25 \text{ }^\circ\text{C}$), a highly ordered texture was obtained (Figure 3d). One should note that during in situ investigation, the precursor nuclei appeared in a short time so that

its formation from the assembly of molecular chains cannot be directly observed. To figure out what happened at the molecule scale, a molecular dynamics (MD) simulation was conducted with seventy P(VDF-TrFE) molecular chains randomly located on the graphene/Cu(122) surface (Figure 3e; Video S1, Supporting Information). Dynamical relaxation of the molecules on the surface was investigated within 1 ns at 298 K. During this process, it was found that most of the molecular chains were first organized into nuclei consisting of six to seven molecular chains with a short-range order after 175 ps (Figure 3f). Subsequently, these small nuclei gradually adjusted their orientations so as to attach to each other and form bands with a longer range before 300 ps (Figure 3g). Upon prolonged relaxation time to 1000 ps, the highly ordered intermittent band structures were formed through the ordering of molecular chains (Figure 3h), which were aligned into parallel arrays and serve as the basic units for the P(VDF-TrFE) lamellae. During this molecule ordering process, the variation in the total energy of this system (Figure S8, Supporting Information) was dominated by the electrostatic energy (Figure 3i) and gradually decreased until the molecules arranged into a stable geometry. These results confirm that such molecular ordering is mainly driven by an electrostatic interaction with the substrate, leading to a large-area textured film within a critical thickness.

The results described above have more general implications for ordered arrangements of other polar molecules on the graphene/Cu(122) via the electrostatic interactions. To verify these implications, different molecules, such as $\text{CH}_3\text{NH}_3\text{PbI}_3$, polypeptides, and N-Boc-N'-Cbz-L-Lysine, have been explored. In

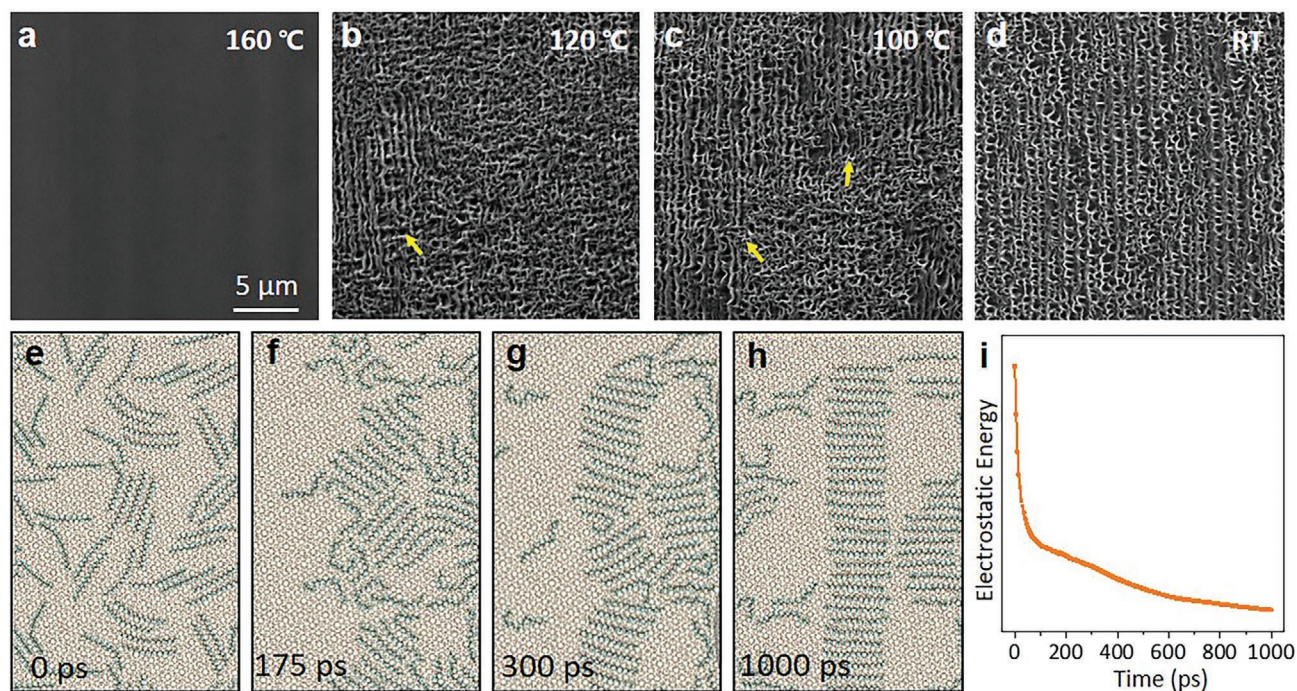


Figure 3. In situ SEM observations and MD simulation of P(VDF-TrFE) on graphene/Cu(122) substrate. a–d) In situ SEM images of P(VDF-TrFE) ordering process on graphene/Cu(122) with temperature decreased. The yellow arrows point to the initial oriented clusters. e–h) Partial snapshots of MD simulation of P(VDF-TrFE) dynamical assembling process on graphene/Cu(122) substrate at different time. i) Electrostatic energy-simulated time curve for the evolution of the molecular arrangement in MD simulation.

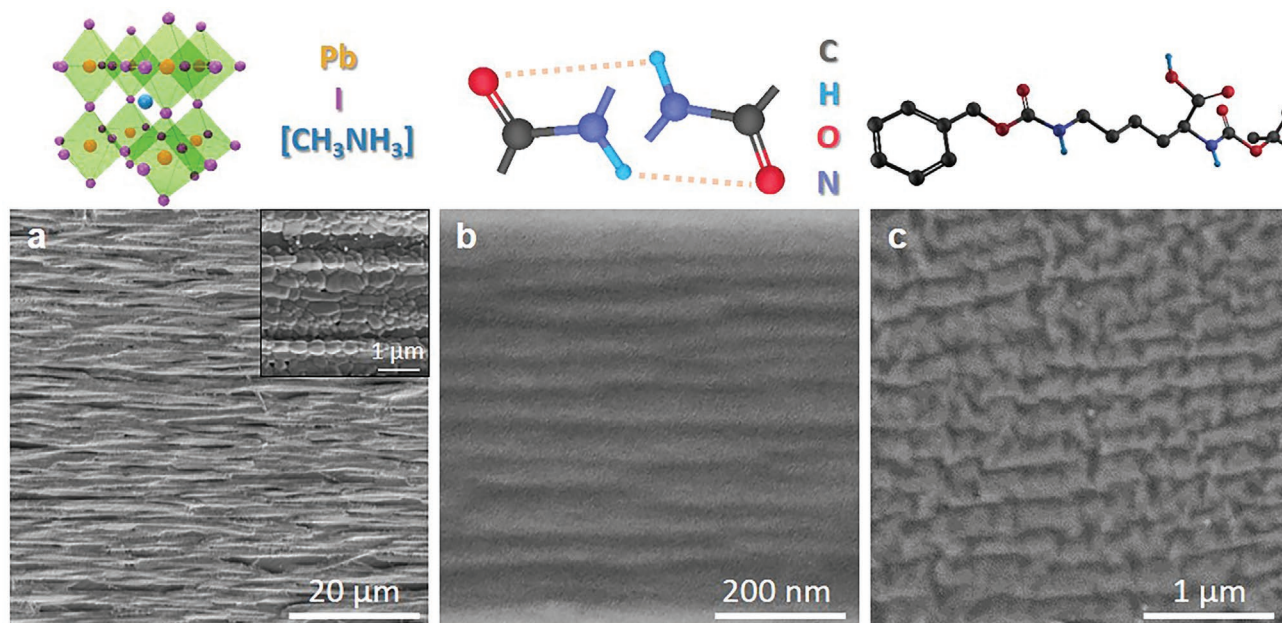


Figure 4. Fabrication of other molecules on graphene/Cu(122) substrate. a–c) SEM images of $\text{CH}_3\text{NH}_3\text{PbI}_3$ (a), polypep low viscosity (b), and Boc- N' -Cbz-L-Lysine (c) grown on graphene/Cu(122) substrates, respectively. The inset of (a) is the high-magnification SEM image of the textured $\text{CH}_3\text{NH}_3\text{PbI}_3$ film. The schematics above correspond to the structures of the molecules, and the dashed lines represent the hydrogen bonding in peptide bonds.

particular, the scalable film of $\text{CH}_3\text{NH}_3\text{PbI}_3$ exhibits a highly ordered texture, consisting of unidirectional rod crystals (Figure 4a, $\approx 2 \mu\text{m}$ in width, $\approx 20 \mu\text{m}$ in length). Interestingly, the arrangement of nanoparticles in the arrayed crystals has preferred (110) lattice planes, indicated by the evidence of XRD pattern (Figure S9a, Supporting Information). Moreover, an obvious arrayed configuration of the polypeptide and N-Boc- N' -Cbz-L-Lysine crystals can be observed on the substrate (Figure 4b,c; Figure S9b, Supporting Information). We attribute these interesting structures to the spontaneous polarization of $\text{CH}_3\text{NH}_3\text{PbI}_3$,^[28] hydrogen bonding from peptide bonds in polypeptides and amino acids,^[8] which is easily regulated by the patterned potential on the substrates within the effective range of electrostatic interactions. As a comparison, no ordered structures have been observed when the films were grown on Cu(122) (Figure S9c–e, Supporting Information).

In summary, our theoretical and experimental results demonstrate the graphene/high-index faceted Cu substrate with a 1D patterned potential on the surface is capable of directing the macromolecule ordering and preparing highly ordered macroscopic films. This platform also provides an opportunity to understand molecular ordering dynamics and mechanism at different scales, which is particularly desirable for organizing molecules into artificial structures in a controlled manner for actual functionalities and devices.^[29] In a broader perspective, the findings may also be applicable to design and construct mixed-dimensional van der Waals heterostructures through noncovalent interactions on the surface of 2D materials.^[30] In addition, the ability to drive the ordering of molecules on the substrate in a long distance would allow to produce highly ordered composite materials consisting of molecule-grafted nanoparticles.^[31] In the meantime, the facile method to prepare macromolecular films with superior performance at large scale

will undoubtedly promote their industrial applications and also expand the application fields.

Experimental Section

Preparation of Graphene/Cu(122) Foils: Large-size single-crystal Cu(122) was prepared by annealing commercial polycrystalline Cu foils (25 μm thick, 99.8%, Sichuan Oriental Stars Trading Co. Ltd.) with a designed “seeded abnormal grain growth” technique. The polycrystalline Cu foil was placed on a quartz substrate with a small piece of single-crystal Cu(122) on its top surface as a seed and loaded into a chemical vapor deposition system. Then the system was heated up to 1020 $^\circ\text{C}$ in 1 h with 800 sccm Ar and 50 sccm H_2 at atmospheric pressure, followed by an annealing process for several hours at the same atmosphere to transform the polycrystalline Cu into Cu(122). After that, continuous graphene film was grown on Cu(122) by introducing CH_4 as carbon source. Finally, stop the CH_4 feeding and let the system cool down naturally.

Growth of P(VDF-TrFE) Thin Films: The P(VDF-TrFE) copolymer (commercial, the mole ratio of VDF to TrFE is 75/25) powder was dissolved into tetrahydrofuran at a range of 5 wt% by stirring at room temperature to produce a clear solution, which were then spin-coated onto different substrates (graphene/Cu(122), graphene/Cu(111), Cu(122), and ITO glass). The thickness of the films can be adjusted by controlling spin-coating parameters. For a typical spin-coating setting, 500 rpm for 3 s and then 1500 rpm for 30 s, the P(VDF-TrFE) films were supposed to have a thickness of 1000 nm. Subsequently, the films on substrates were dried and annealed in a vacuum oven at 180 $^\circ\text{C}$ for 2 h.

Transfer of P(VDF-TrFE) Thin Films: The as-grown P(VDF-TrFE) thin film was transferred by Cu-etched method.^[32] An ammonium persulfate ($(\text{NH}_4)_2\text{S}_2\text{O}_8$, 1 M, Sigma-Aldrich) solution was used to etch the Cu away, and then the freestanding thin film was rinsed by deionized water five times. Subsequently, the floating P(VDF-TrFE) thin film was transferred onto ITO glass, and dried in air.

Growth of $\text{CH}_3\text{NH}_3\text{PbI}_3$ Films: $\text{CH}_3\text{NH}_3\text{I}$ (0.200 g, Macklin) and PbI_2 (0.578 g, Macklin) were dissolved in anhydrous N,N -dimethylformamide

(1 mL, Macklin) by stirring at room temperature to produce a clear solution with concentration of 45 wt%. Then the solution was spin-coated onto different substrates (graphene/Cu(122), Cu(122)), and the spin-coating parameter was set at 1500 rpm for 3 s and 5000 rpm for 30 s. The obtained films were dried in a vacuum oven at 100 °C for 10 min.^[33]

Growth of Crystals of Polyep Low Viscosity: Polyep low viscosity (1.000 g, Sigma-Aldrich) was dissolved in anhydrous *N,N*-dimethylformamide (20 mL, Macklin) by stirring at room temperature to produce a clear solution. The solution was dropped onto different substrates (graphene/Cu(122), Cu(122)) and the spin-coating parameter was set at 1000 rpm for 3 s and 3000 rpm for 30 s. The obtained samples were dried at room temperature.

Growth of *N*-Boc-*N'*-Cbz-*L*-Lysine Crystals: *N*-Boc-*N'*-Cbz-*L*-Lysine (0.579 g, Jiedingchem) was dissolved in anhydrous *N,N*-dimethylformamide (20 mL, Macklin) by stirring at room temperature to produce a clear solution. *N*-Boc-*N'*-Cbz-*L*-Lysine solution was dropped onto different substrates (graphene/Cu(122), Cu(122)) and the spin-coating parameter was set at 1000 rpm for 3 s and 3000 rpm for 30 s. The obtained samples were dried at room temperature.

Morphology and Structure Characterizations: EBSD characterization of Cu foil was carried out by field-emission SEM (Zeiss Merlin) and XRD was conducted using a Bruker D8 Advance system with a silver target ($\lambda = 0.56 \text{ \AA}$). The morphology and structure of P(VDF-TrFE) thin films were characterized by SEM (Hitachi SU70) and XRD (Cu $K\alpha$ radiation, $\lambda = 1.54056 \text{ \AA}$). The thickness was detected by a step profiler (DEKTA-XT, Bruker, America). The DSC curve was recorded by differential scanning calorimeter (DSC Q100 V9.7 Build 291).

GIWAXS Measurements: GIWAXS measurements were carried out with an Xeuss 2.0 SAXS/WAXS laboratory beamline using a Cu X-ray source (8.05 keV, 1.54 Å) and a Pilatus 3R 300K detector. The P(VDF-TrFE) thin film on the graphene/Cu substrate was placed in the center of the stage. The stage was controlled by a motor to change the in-plane rotational angle of the sample. The incidence angle is 0.2°.

In Situ SEM Observation: The in situ ordering process was observed using an FEI Quanta 650 environment scanning electron microscope equipped with a 1000 °C heating stage. P(VDF-TrFE) was first spin-coated on the graphene/Cu(122) substrate with solvent evaporated under vacuum at room temperature. Subsequently, the sample was heated to 160 °C with heating rate 30 °C min⁻¹, hold for 30 min, and then cooled.

Molecular Dynamics Simulations: MD simulation method for the ordering process of P(VDF-TrFE) molecular chains on graphene/Cu(122) substrate was based on the COMPASS force field using the molecular mechanics tool Forcite.^[34] The orientation relationship between the graphene layer and Cu(122) surface was determined by the geometry optimization of a system consisting of a graphene flake and Cu(122) surface. As for a specific setup of MD simulation, a 1 fs time step has been taken under 298 K in NVT ensemble with a total simulation time of 1 ns, a consensus that is generally believed a long enough period to contain necessary transition states of molecular arrangement.

Density Functional Theory Calculations: The DFT calculations were carried out with the Cambridge Serial Total Energy Package in the plane-wave basis and within the projector-augmented wave description of the core regions. The Perdew, Burke, and Ernzerhof exchange-correlation function was adopted in the calculations, which were all done within the generalized gradient approximation, with cut-off energy of 353.7 eV. For the structure models, a Cu(122)/graphene supercell was built by covering the Cu(122) surface with a graphene monolayer.

Property Measurements: P(VDF-TrFE) films were transferred to conductive ITO substrate and the equipment for mechanical measurement with copper substrates being etched. Ferroelectric property was measured at 100 Hz by RT66A ferroelectric tester (Radiant Technologies Inc., Albuquerque, NM, USA). The mechanical property was measured by Instron 5943.

Supporting Information

Supporting Information is available from the Wiley Online Library or from the author.

Acknowledgements

The authors acknowledge the financial support from the National Natural Science Foundation of China (Grant Nos. U1909212, U1809217, 21771161, and 51991342), the Natural Science Foundation of Zhejiang Province (LR21E020004), the Key R&D Program of Zhejiang Province (2020C01124), the Zhejiang Provincial Natural Science Foundation of China (Grant No. LR18B030003), the financial support from Research Grant Council of Hong Kong (General Research Fund No. 24306318), the Key R&D Program of Guangdong Province (2020B010189001 and 2019B010931001), Bureau of Industry and Information Technology of Shenzhen (Graphene platform 201901161512), and the Thousand Talents Program for Distinguished Young Scholars.

Conflict of Interest

The authors declare no conflict of interest.

Author Contributions

D.K.Z., Z.H.Z., and Y.H.Z. contributed equally to this work. Z.H.R. and K.H.L. initiated the work. Z.H.R., K.H.L., X.H.L., and G.R.H. supervised the work. D.K.Z., Z.H.Z., Y.R.S., and Z.B.Z. synthesized the samples. D.K.Z., Z.H.Z., Z.H.R., K.H.L., and X.H.L. analyzed the data and wrote the manuscript. D.K.Z., Z.H.Z., and L.Y.R. characterized the microstructure. Y.H.Z., G.S., and C.Z.Z. performed the MD and DFT simulations. Y.Q.X. conducted GIWAXS experiments. Q.Q.D. and J.X.L. carried out the in situ SEM experiment. Y.J.W. and Y.H.H. gave advice to improve the samples. Z.P.C., D.P.Y., E.G.W., and G.R.H. revised the manuscript. All the authors participated in the analysis and discussion.

Data Availability Statement

The data that support the findings of this study are available from the corresponding author upon reasonable request.

Keywords

graphene/high-index Cu substrates, high ordering, large scale film growth, macromolecular films, patterned potentials

Received: October 8, 2020

Revised: March 31, 2021

Published online: June 6, 2021

- [1] T. Someya, Z. N. Bao, G. G. Malliaras, *Nature* **2016**, *540*, 379.
- [2] J. F. Patrick, M. J. Robb, N. R. Sottos, J. S. Moore, S. R. White, *Nature* **2016**, *540*, 363.
- [3] Y. Lei, Y. Chen, R. Zhang, Y. Li, Q. Yan, S. Lee, Y. Yu, H. Tsai, W. Choi, K. Wang, Y. Luo, Y. Gu, X. Zheng, C. Wang, C. Wang, H. Hu, Y. Li, B. Qi, M. Lin, Z. Zhang, S. A. Dayeh, M. Pharr, D. P. Fenning, Y. H. Lo, J. Luo, K. Yang, J. Yoo, W. Nie, S. Xu, *Nature* **2020**, *583*, 790.
- [4] E. Kopperger, J. List, S. Madhira, F. Rothfischer, D. C. Lamb, F. C. Simmel, *Science* **2018**, *359*, 296.
- [5] M. Ouchi, N. Badi, J. F. Lutz, M. Sawamoto, *Nat. Chem.* **2011**, *3*, 917.
- [6] M. Guo, J. Jiang, J. Qian, C. Liu, J. Ma, C. W. Nan, Y. Shen, *Adv. Sci.* **2019**, *6*, 1801931.

- [7] K. C. K. Cheng, M. A. Bedolla-Pantoja, Y.-K. Kim, J. V. Gregory, F. Xie, A. de France, C. Hussal, K. Sun, N. L. Abbott, J. Lahann, *Science* **2018**, *362*, 804.
- [8] K. Tao, P. Makam, R. Aizen, E. Gazit, *Science* **2017**, *358*, eaam9756.
- [9] T. P. Knowles, T. W. Oppenheim, A. K. Buell, D. Y. Chirgadze, M. E. Welland, *Nat. Nanotechnol.* **2010**, *5*, 204.
- [10] S. A. Tofail, J. Bauer, *Adv. Mater.* **2016**, *28*, 5470.
- [11] K. B. Blodgett, *J. Am. Chem. Soc.* **1935**, *57*, 1007.
- [12] M. Aryal, K. Trivedi, W. Hu, *ACS Nano* **2009**, *3*, 3085.
- [13] Y. Diao, B. C. Tee, G. Giri, J. Xu, D. H. Kim, H. A. Becerril, R. M. Stoltenberg, T. H. Lee, G. Xue, S. C. Mannsfeld, Z. Bao, *Nat. Mater.* **2013**, *12*, 665.
- [14] J. V. Barth, G. Costantini, K. Kern, *Nature* **2005**, *437*, 671.
- [15] W. Yang, G. Chen, Z. Shi, C. C. Liu, L. Zhang, G. Xie, M. Cheng, D. Wang, R. Yang, D. Shi, K. Watanabe, T. Taniguchi, Y. Yao, Y. Zhang, G. Zhang, *Nat. Mater.* **2013**, *12*, 792.
- [16] K. Xiao, W. Deng, J. K. Keum, M. Yoon, I. V. Vlassiok, K. W. Clark, A. P. Li, I. I. Kravchenko, G. Gu, E. A. Payzant, B. G. Sumpter, S. C. Smith, J. F. Browning, D. B. Geohegan, *J. Am. Chem. Soc.* **2013**, *135*, 3680.
- [17] X. Xu, Z. Zhang, J. Dong, D. Yi, J. Niu, M. Wu, L. Lin, R. Yin, M. Li, J. Zhou, S. Wang, J. Sun, X. Duan, P. Gao, Y. Jiang, X. Wu, H. Peng, R. S. Ruoff, Z. Liu, D. Yu, E. Wang, F. Ding, K. Liu, *Sci. Bull.* **2017**, *62*, 1074.
- [18] L. Wang, X. Z. Xu, L. N. Zhang, R. X. Qiao, M. H. Wu, Z. C. Wang, S. Zhang, J. Liang, Z. H. Zhang, Z. B. Zhang, W. Chen, X. D. Xie, J. Y. Zong, Y. W. Shan, Y. Guo, M. Willinger, H. Wu, Q. Y. Li, W. L. Wang, P. Gao, S. W. Wu, Y. Zhang, Y. Jiang, D. P. Yu, E. G. Wang, X. D. Bai, Z. J. Wang, F. Ding, K. H. Liu, *Nature* **2019**, *570*, 91.
- [19] X. Xu, Z. Zhang, L. Qiu, J. Zhuang, L. Zhang, H. Wang, C. Liao, H. Song, R. Qiao, P. Gao, Z. Hu, L. Liao, Z. Liao, D. Yu, E. Wang, F. Ding, H. Peng, K. Liu, *Nat. Nanotechnol.* **2016**, *11*, 930.
- [20] M. Wu, Z. Zhang, X. Xu, Z. Zhang, Y. Duan, J. Dong, R. Qiao, S. You, L. Wang, J. Qi, D. Zou, N. Shang, Y. Yang, H. Li, L. Zhu, J. Sun, H. Yu, P. Gao, X. Bai, Y. Jiang, Z. J. Wang, F. Ding, D. Yu, E. Wang, K. Liu, *Nature* **2020**, *581*, 406.
- [21] C. Lin, X. Huang, F. Ke, C. Jin, N. Tong, X. Yin, L. Gan, X. Guo, R. Zhao, W. Yang, E. Wang, Z. Hu, *Phys. Rev. B* **2014**, *89*, 085416.
- [22] P. A. Khomyakov, G. Giovannetti, P. C. Rusu, G. Brocks, J. van den Brink, P. J. Kelly, *Phys. Rev. B* **2009**, *79*, 195425.
- [23] S. Zhang, *Nat. Biotechnol.* **2003**, *21*, 1171.
- [24] I. Š. Rakić, M. Kralj, W. Jolie, P. Lazic, W. H. Sun, J. Avila, M. C. Asensio, F. Craes, V. M. Trontl, C. Busse, P. Pervan, *Carbon* **2016**, *110*, 267.
- [25] J. H. Kang, J. Moon, D. J. Kim, Y. Kim, I. Jo, C. Jeon, J. Lee, B. H. Hong, *Nano Lett.* **2016**, *16*, 5993.
- [26] J. Liu, J. Q. Mai, S. Li, Z. H. Ren, M. Li, M. J. Wu, Y. J. Wu, X. H. Lu, X. Li, H. Tian, Z. R. Wang, G. R. Han, *Acta Phys. - Chim. Sin.* **2017**, *33*, 1261.
- [27] Y. C. Wu, J. K. Yim, J. M. Liang, Z. C. Shao, M. J. Qi, J. W. Zhong, Z. H. Luo, X. J. Yan, M. Zhang, X. H. Wang, R. S. Fearing, R. J. Full, L. W. Lin, *Sci. Rob.* **2019**, *4*, 1594.
- [28] H. S. Kim, S. K. Kim, B. J. Kim, K. S. Shin, M. K. Gupta, H. S. Jung, S. W. Kim, N. G. Park, *J. Phys. Chem. Lett.* **2015**, *6*, 1729.
- [29] J. J. Chen, E. B. Zhu, J. Liu, S. Zhang, Z. Y. Lin, X. F. Duan, H. Heinz, Y. Huang, J. J. De Yoreo, *Science* **2018**, *362*, 1135.
- [30] D. Jariwala, T. J. Marks, M. C. Hersam, *Nat. Mater.* **2017**, *16*, 170.
- [31] C. Yi, Y. Yang, B. Liu, J. He, Z. Nie, *Chem. Soc. Rev.* **2020**, *49*, 465.
- [32] Y. F. Hao, M. S. Bharathi, L. Wang, Y. Y. Liu, H. Chen, S. Nie, X. H. Wang, H. Chou, C. Tan, B. Fallahazad, H. Ramanarayan, C. W. Magnuson, E. Tutuc, B. I. Yakobson, K. F. McCarty, Y. W. Zhang, P. Kim, J. Hone, L. Colombo, R. S. Ruoff, *Science* **2013**, *342*, 720.
- [33] M. Xiao, F. Huang, W. Huang, Y. Dkhissi, Y. Zhu, J. Etheridge, A. Gray-Weale, U. Bach, Y. B. Cheng, L. Spiccia, *Angew. Chem., Int. Ed.* **2014**, *53*, 9898.
- [34] S. W. Bunte, H. Sun, *J. Phys. Chem. B* **2000**, *104*, 2477.